METHODS FOR REAL-TIME VISUALIZATION AND EXPLORATION IMPROVEMENTS OF PRECIPITATION RADAR AND TEMPERATURE DATA IN WEB-CARTOGRAPHY

Christophe Lienert
lienert@karto.baug.ethz.ch

Melanie Kunz
kunz@karto.baug.ethz.ch

Lorenz Hurni
hurni@karto.baug.ethz.ch

Institute of Cartography
ETH Zurich
8093 Zurich, Switzerland

Rolf Weingartner
Geographical Institute
University of Berne
3012 Berne, Switzerland
wein@giub.unibe.ch

Abstract

Most private or public weather service providers deliver their precipitation radar data on the web in form of ill-colored, static raster images. Applied coloring, contrast levels and the number of data classes disallow easy legibility of precipitation quantities. Hardly any interaction between users and data is provided, which could partly derestrict these shortcomings. Temperature data, in turn, are often confined to point data representations without spatial distribution. Or they are represented as non-interactive, interpolated raster images with too many class numbers. In this paper, methods are proposed that tackle these problems in real-time, using true real-time data from network operators. Automated work flows are proposed to improve legibility of precipitation radar images. Also, automations are shown that result in temperature maps covering comparable point, interpolated line and area map symbolizations. Within these work flows, radar and temperature maps are further provided with interactive functionalities to facilitate data exploration. The results are built into an operational, web-based cartographic application.

1. Introduction

1.1. Users and Needs

Real-time and automatically updated precipitation and temperature data are two main indispensable parameters in flood management and early warning. Temperature data, particularly the position of the 0°C isotherm combined with the areal distribution of precipitation is crucial to distinguish the area on which precipitation either falls in liquid or frozen form. As snow delays runoff and melt water may considerably contribute to flooding, the temperature distribution critically determines a basin's runoff disposition. By combining precipitation radar and areal temperature distribution in form of well-readable, interactive real-time web map composites, flood specialists are supported in their decision making before and during severe flood events.

1.2. Background on Precipitation Radar and Temperature Interpolation

First generation weather radars in the 1960s used to be qualitative, stand-alone products, geared towards one single user. With the advancement of technology and user-oriented research, the monitoring aspect has become more important. Since the 1990s weather radars have been refined to generate integrated, quantitative products to a wide range of users. Today, various hydro-meteorological parameters are analyzed, processed and dispatched in sophisticated end-to-end systems (see examples in Fig. 1). Information extractable from weather radars encompass the identification of the precipitation's consistency (ice, snow, sleet, rain), thunderstorm nowcasting, storm tracking, wind monitoring and quantitative precipitation estimation. Latter is – either in combination with, or separate from, ground precipitation gauges – used as input of hydrological models (e.g., Fang *et al.* 2008; Germann *et al.* 2009). Estimation of precipitation amounts, however, is fraught with substantial uncertainties. Several instrumental and meteorological factors affect the accuracy of radar estimates (Chumchean *et al.* 2006; Germann *et al.* 2006). When measuring precipitation, the radar uses its own wave's backscatter signals caused by hydrometeors in the atmosphere. Owing to this indirect measurement method and other related difficulties, the main advantage of radar still remains its capability to indicate, in real-time and high-resolution, the extent of a precipitation field over a large area (rather than measuring precise quantities).

For air temperature, different interpolation methods exist to estimate those values that are intermediate to observations made at single points. The methods' accuracy is depending on the accuracy of the observations themselves, the density of both observation and validation points, and the spatial variability of the terrain's surface (e.g., MacEachren and Davidson 1987; Szentimrey *et al.* 2007). The choice of the used interpolation scheme determines the quality of the results, particularly in mountainous regions. Here, observation sites are sparse and temperature changes are substantial due to small-scale changes in elevation. Yet, not only spatial but also temporal resolution of temperature data has an impact on the interpolation model performance. Hourly

temperatures tend to show increased variability as opposed to daily or even monthly means. The inclusion of solar radiance data to common lapse rate-corrected inverse distance weighting interpolation models seems to be a promising approach to better explain the temporal variability of temperature (e.g., Chung and Yun 2004; Huang *et al.* 2008; Wratt *et al.* 2006).

1.3. Related Developments in Real-Time Web-Cartography

Presenting data in web maps requires an effective design that balances form and function of the map. Incorporated in a graphical user interface and linked to different functionalities, users may make the most out the map if they are enabled to modify its content and symbolization. In contrast to printed maps, web maps provide for a more comprehensive information communication and enhanced cartographic exploration and analysis (Cartwright 2003). But graphical design of digital web maps must imperatively be geared towards straightforward legibility. This, in turn, requires the consideration of basic cartographic design principles (e.g., avoidance of information ambiguities).

Several other research projects in the domain of natural hazard and forecasting increasingly tend to focus on the rapid mapping and real-time visualization part of their real-time and archived data (e.g., Haubrock *et al.* 2008; Hegg and Rhyner 2007). Therefore, aspects of online and fully-automated accomplishment of cartographic work steps become more and more important. Works steps may include the acquisition, storage, processing, visual abstraction, front-end visualization and archiving of raw real-time data (Lienert *et al.* 2007).

1.4. Outline of the Paper

A comprehensive concept to generate cartographic real-time products for operational hydrology has been designed prior to the partial project presented here. Various proofs of this concept have been discussed (Lienert *et al.* 2009). Based on a fully-fledged technical framework, emphasis of this paper is on the methodology to visually improve and interactively enhance exploration of real-time radar and temperature data.

The objectives of the work are stated in the following section, with respect to the above mentioned user needs. Use cases of web-based radar images and temperature maps are discussed in view of their visual and data exploration shortcomings. The methodology section refers to a conceptual workflow (Fig. 3) and highlights each processing step that is passed through in real-time. The output maps are discussed in the result section. Their advantages over existing solutions, as well as remaining improvement options, are taken up in the discussion and conclusion section.

2. Objectives

2.1. Improving the Display and Access of Real-Time Precipitation Radar Data

Coloring of *radar* image products is not standardized and radar images on the web are often difficult to read as they fail to observe basic cartographic rules: coloring is unsuitable for quantitative data and data class numbers are often too large. Users are overwhelmed and are likely to miss out on seeing possible trends or spatial patterns (see, e.g., Slocum 2009). Fig. 1 shows four examples of online published radar maps. Merely the one on top left was made with a suitable, albeit maximal, class number. All other examples, especially the one on the bottom right, are equipped with too many classes, making them difficult to read. Also, the used color schemes of all examples rather resemble qualitative than quantitative data. Since we deal with precipitation depths ([mm] or [in] within a given time interval), a sequential color scheme with varying lightness and unchanged hue is more applicable (Brewer *et al.* 2003). Although partly applied in the examples top right and bottom left of Fig. 1, these schemes use different hues from a certain threshold. In addition to color related problems, the radar images, especially the one on bottom left, appear much too coarse. Some visual smoothing would more genuinely represent the cloudy character of the precipitation fields.

As a consequence, the objective for precipitation radar data is to develop processes that reclassify and recolor each grid cell from the original data according to a quantitative color scheme with reduced data classes.

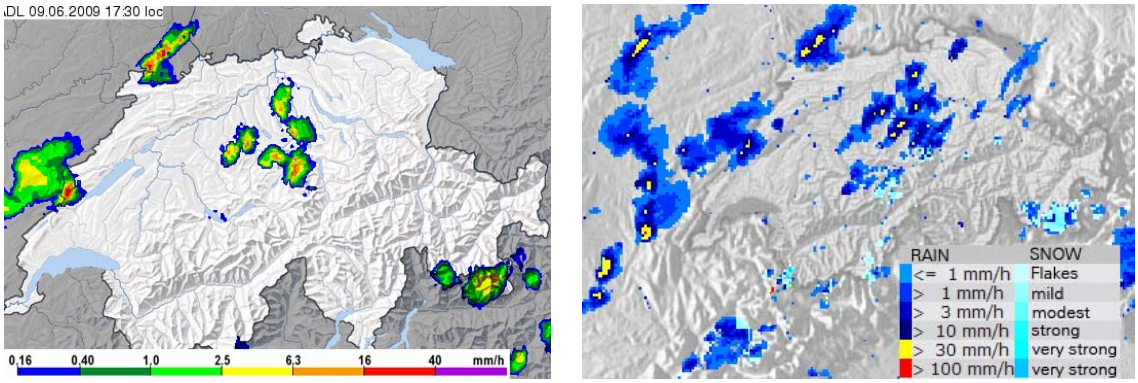

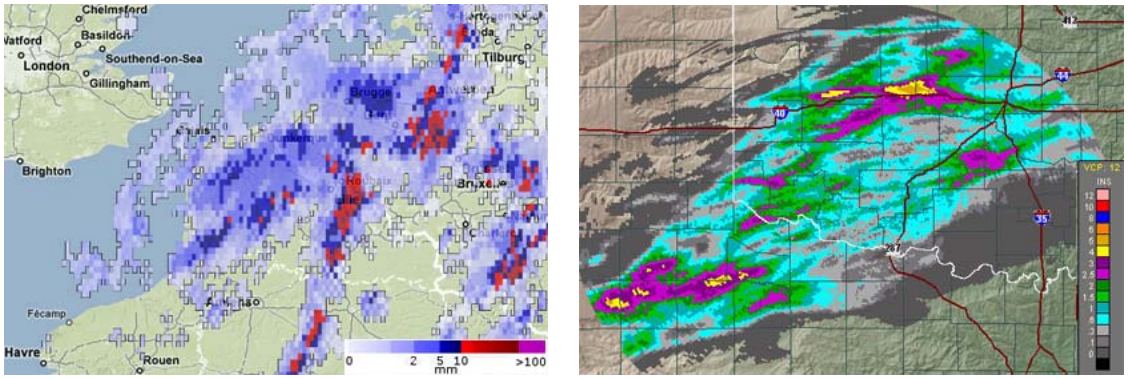

Fig. 1. Examples of online precipitation radar maps (Sources: sma.ch, sf.tv, weather.gov, meteox.com, clockwise from top left)

2.2. Offering Additional Visualization from Real-Time Point Temperature Data

Temperature data is measured and sent to the network operator's central databases with advanced sensor-logger-telecommunication technology. They are measured at particular locations. Well-readable point symbolizations, combined with quick numerical display may effectively communicate temperature data. When mapping areal temperature distributions, adequate cartographic design is needed that allows the display of additional data (such as precipitation radar). Examples of temperature maps are given in Fig. 2. On the left, measured values are located at the gauging sites and mapped on top of the interpolated temperature surface. This temperature map provides a good-looking overview of the temperature situation. Yet, it lacks a corresponding legend and the feasibility of overlapping additional area symbolizations is problematic. In the right example of Fig. 2, temperature is represented by simple, uniform dots along with the numerical indication of the measured values. In this case, the map might be complemented by a radar raster image without compromising legibility, but areal temperature distribution representation is missing. Besides, no interaction with the user is provided for both examples.

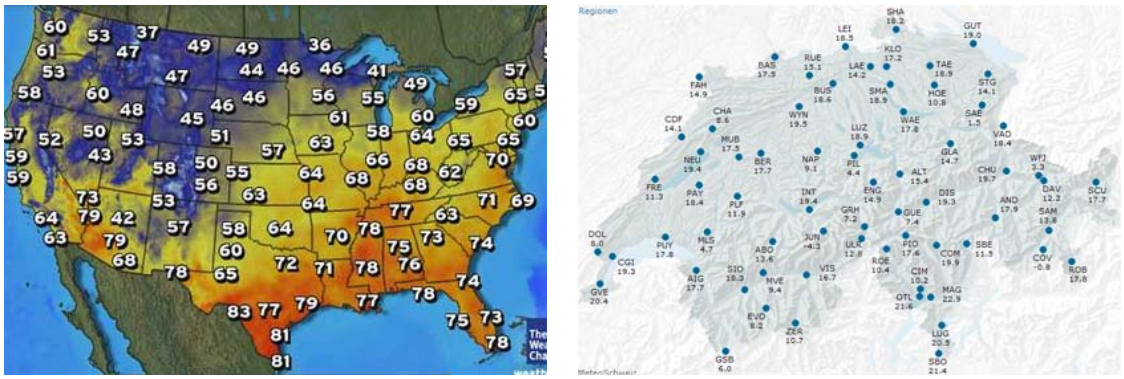

Fig. 2. Examples of online temperature maps (weather.com, sma.ch, left to right)

The objective for temperature data is to offer more, easily switchable visualizations. These should be combinable with the radar, but not affect its legibility. To this end, three different visualizations are needed: First, suitable point symbolization must be designed. Next, functions must be developed, capable of interpolating real-time point data to a temperature surface raster. A diverging color scheme will be applied to this surface. Lastly, the 0°C isotherm must be extracted from the interpolated surface. The isotherm allows for distinguishing areas below and above the freezing point. It will also facilitate the combination of radar and temperature data without adversely affecting map legibility.

2.3. Improving Data Exploration of Generated Radar and Temperature Maps

Many radar and temperature maps published on private or public weather service sites are presented in form of static images. Interaction between users and maps is hardly provided, though this could substantially facilitate data exploration and ensure that all information is conveyed to the user. The objective is to improve data exploration by developing functions that retrieve the values of the generated raster image. Each pixel of the image should therefore be associated with its underlying value and linked to an appertaining legend.

3. Methodology

3.1. Used Data

In the presented project, workflows are tested with true real-time data provided by the *Swiss Federal Office of Meteorology and Climatology*. Results are accessible in a web-based graphical user interface. The raw data is read out from files transferred by the network operator. The operator receives measurements in real-time from the sensors and caches them on its own servers before passing them on to the server of this project.

3.2. Real-time Workflow and Functions for Precipitation Radar Data

Schematic real-time workflows including processing, visualization and exploration functions were devised and implemented. The workflow and resulting output for both radar and temperature data is shown in Fig. 3. In this section, those processes relevant for radar data are discussed:

Box A: Radar data arrives hourly via FTP in a supplier-specific binary format. Essentially, it is a GIF file with header information and therefore not web-enabled.

Box B: Initial image processing functions handle the bit input streaming and read out the radar's time of measurement at an invariant position in the file (function named *readFromRadar)*. The more complex *radarConverter* function is the core of the radar

image processing. As from the invariant date position of the buffered stream, each pixel is looped through and checked for its actual RGB value. These RGB values are replaced by new ones and complemented by an alpha channel. The original black background of the radar image, for example, is replaced by a color with the alpha channel set to zero (and made transparent, respectively). The modified file is then resized and converted to a GIF as well as a PNG format. Both files are each named after the associated timestamp and as "actual". This way, the most actual file is overwritten and easily addressable by this name, while a copy of it is saved in the archive. The full path of the archive copy is stored in the radar table of the database, using the *writePath2DB* function. The path is later used for other purposes.

Box C: Grid functions create grid files that contain the indexed color values of the above generated PNG. To achieve this, the function *gdal_translate* uses the auxiliary created GIF file and translates it into an ASC file. This file now contains the indexed colors of the GIF (GDAL 2009). Using the PNG for this translation instead may seem more practical. It is possible but problematic since the *gdal_translate* function requires one, specified color band of the PNG. Regardless of which band of the radar PNG is passed to the function, the resulting grid will not contain unique values (i.e., assignment of a value to a single color is not possible). Applying the *hierarchicalGrid* function removes the GIF and processes the ASC further to a binary file containing the same indexed color information. Again, two copies of this BIN file are stored: one named after the timestamp and one called "actual". The *gridLayer* function passes the actual BIN to an in-built web-service that returns the indexed color in an XML-format. These index values are later used to generate the legend when the mouse is moved over the pixels of the raster image. The intermediate creation of the BIN file and the invocation of the web-service within the workflow is essential. This way, all indexed values can be addressed and flexibly handled, regardless of the map scale and the raster data's resolution (HIGRID 2008). Other text-based solutions might be feasible to achieve the same effects (see, e.g., Antoniou and Tsoulos 2006), but have not been tested.

Box D: After the creation of the image and the underlying grid (a process of approx. 1 second), the *rasterLayers* function fetches the raster image by building a URL. Raster data are served over the internet by an in-built web-map server and integrated in the document object model (DOM) of the web map. The PNG image benefits from additional visualization-enhancing *web-map server functions*, such as transparency controlling or bilinear resampling (UMN 2009). Simultaneously, the *gridLayer* function binds the output of the above mentioned grid web-service into the web application in form of an array object (i.e., *not* into the DOM). The corresponding x- and y-coordinates of the visualized raster data are directly associated with the position and the value in the array and, when the mouse is moved, passed to the *showGridValues* function. In this function, so called legend strings are built. They consist of the data class number, the RGB values for each class, and the absolute class interval limits. The grid value determined by the position of the mouse is concatenated to the legend strings

and the function *addOrRemoveLegend* is called. This function creates the dynamic legend on the screen by processing the full, concatenated legend string.

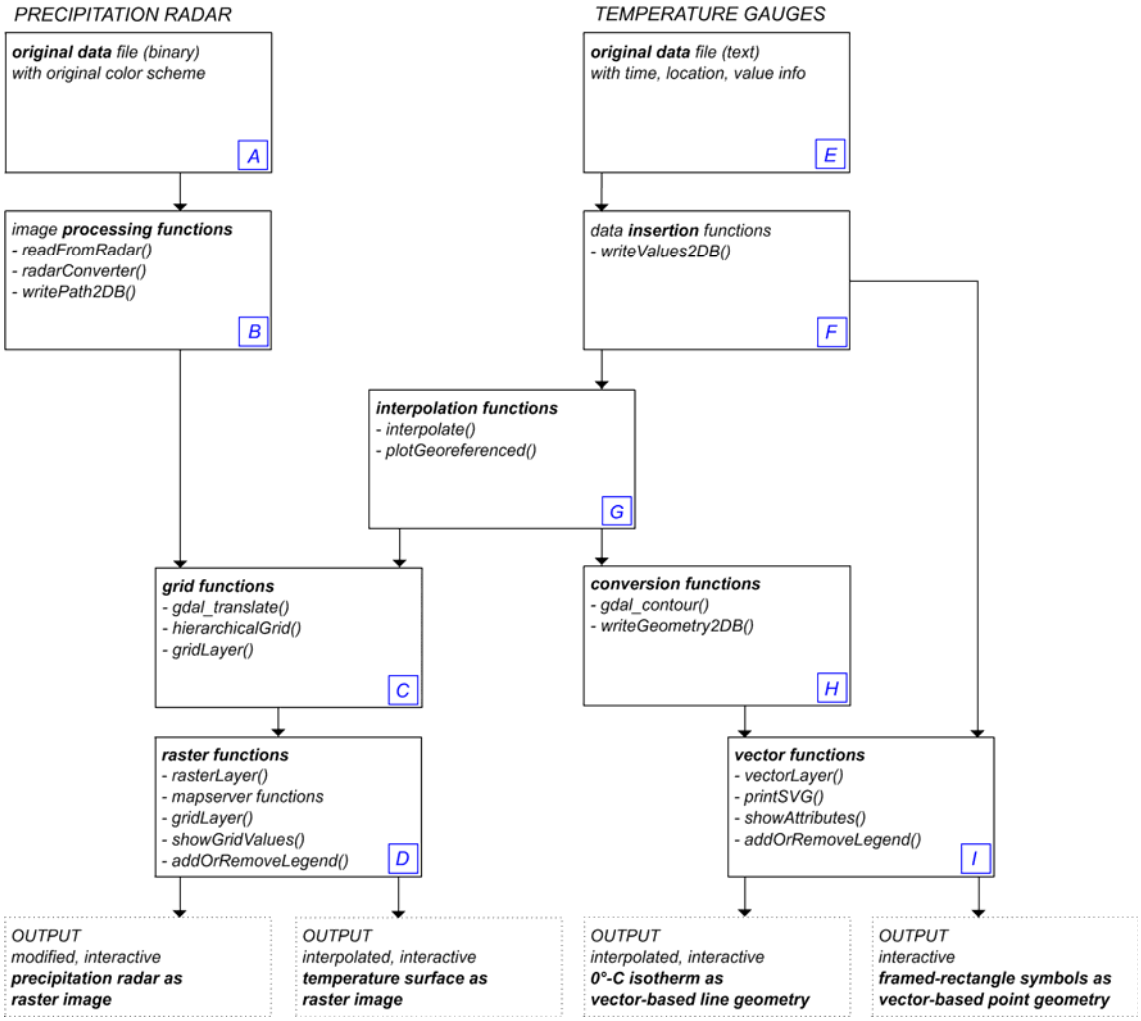

Fig. 3. Schematic real-time workflow for precipitation radar and temperature data

3.3. Real-time Workflow and Functions for Temperature Data

In this section, all associated functions of the workflow concerning the data from temperature gauges are discussed (see Fig. 3).
Box E: Unlike radar data, temperature data arrive via FTP in a human readable text format, containing the time and location of their measurement, and the measured value.

Box F: The timed function *writeValues2DB* inserts measurement values into a database. For every temperature gauge, a table exists to which new data records are appended. The process is complex, but the setup of the whole database and its schemas is part of another, planned paper. In order that no duplicates occur, the time of measurement itself

is defined as the unique identifier (Lienert *et al.* 2009; Valpreda 2004). Rudimentary quality checks are performed on this level (data type, data sign, data range, conversion into placeholder value when no data are delivered). The point geometry representing all the gauging locations of the measurement network is stored in a separate table. Network data is joined with the real-time data, directly resulting in a point map with temperature symbols. These symbols are dynamically generated and their appearance depends on the absolute real-time value (see Fig. 4).

Box G: The *interpolate* function queries real-time (i.e., the most recent) values from each table in the database. Gauges with invalid values are automatically left out for the consecutive steps. Real-time data are joined to the respective gauge location coordinates of the network table. Temperature is then interpolated to all the points intermediate to gauging stations using an inverse distance weighted algorithm on the 0°C level. This level is pre-calculated from the normal, time-independent 0.65°C/100m lapse rate. The lapse rate and a 100x100m elevation grid are then used to calculate back and determine the final interpolated temperature surface. To speed up the process, the interpolation is performed on over 90 individual tiles which are then merged to one large grid. Before it is saved to an ASC file, it is projected. In the *plotGeoreferenced* function, the coloring of the data takes place by creating RGBA bands and applying the new color scheme. After the assignments of colors to each grid value, the file is saved as a high resolution TIFF file (not as a compressed GIF that contains only one color band). The workflow continues with grid creation functions already described above for *Box C*. Then, a PNG is created out of the TIFF. The PNG is then converted into an ASC file by passing the B-band to the *gdal_translate* function. The resulting ASC merely stores the color information of this single B-band. It does not contain indexed color values, as is the case when translating the one-color band radar GIF in to an ASC file. But yet, the B-band values are unambiguously distinguishable and consecutive functions in *Box C* and *Box D* can be applied. Executing all functions in this *Box G* takes well over one minute.

Box H: The resulting ASC file is further processed by the function *gdal_contour*. The complete interpolated ASC is passed to this function along with the elevation for which 0°C is modeled. The contour line of this elevation results in the desired 0°C isotherm vector geometry. The real-time calculation of the 0°C elevation is done with the lapse-rate formula, using an arbitrarily chosen cell on the elevation grid and its associated cell on the temperature grid. The function *writeGeometry2DB* loads the resulting isotherm vector into the spatial database along with its corresponding timestamp and determined 0°C elevation. Executing functions in this *Box H* consume a few seconds.
Box I: Geometry and corresponding attributes (such as the corresponding timestamps) are transferred asynchronously from the server to the browser. The task is accomplished by the *vectorLayer* function. When the data from both *Box H* and *Box F* are fetched from the database, they are printed as Scalable Vector Graphic (SVG) by the *printSVG* function. The printed code is then immediately appended to its designated location within the DOM, and thus visualized in the web browser. Framed rectangles are used to depict the temperature data from *Box F* (see Fig. 4). A rectangle denotes the temperature

range from 0°C to 30°C (or 0°C to minus 30°C, respectively) and frames the colored temperature column. The height of the colored column is proportional to the framing rectangle and is rendered in real-time, using the real-time value fetched from the database. The *printSVG* function also adds the stroke width and stroke color to the 0°C isotherm. Beside visualization of the geometry and map symbols, data attributes are interactively presented to the user by the *showAttributes* function. When the mouse is moved over a framed rectangle or the 0°C isotherm, textual and numerical information is directly worked up from the data supplied by the *printSVG* function. The data are then arranged and displayed either in form of tool tips or in an additional movable and resizeable window. As for raster data, the *addOrRemoveLegend* automatically displays legend information for vector data, using the same procedures as described for *Box D*.

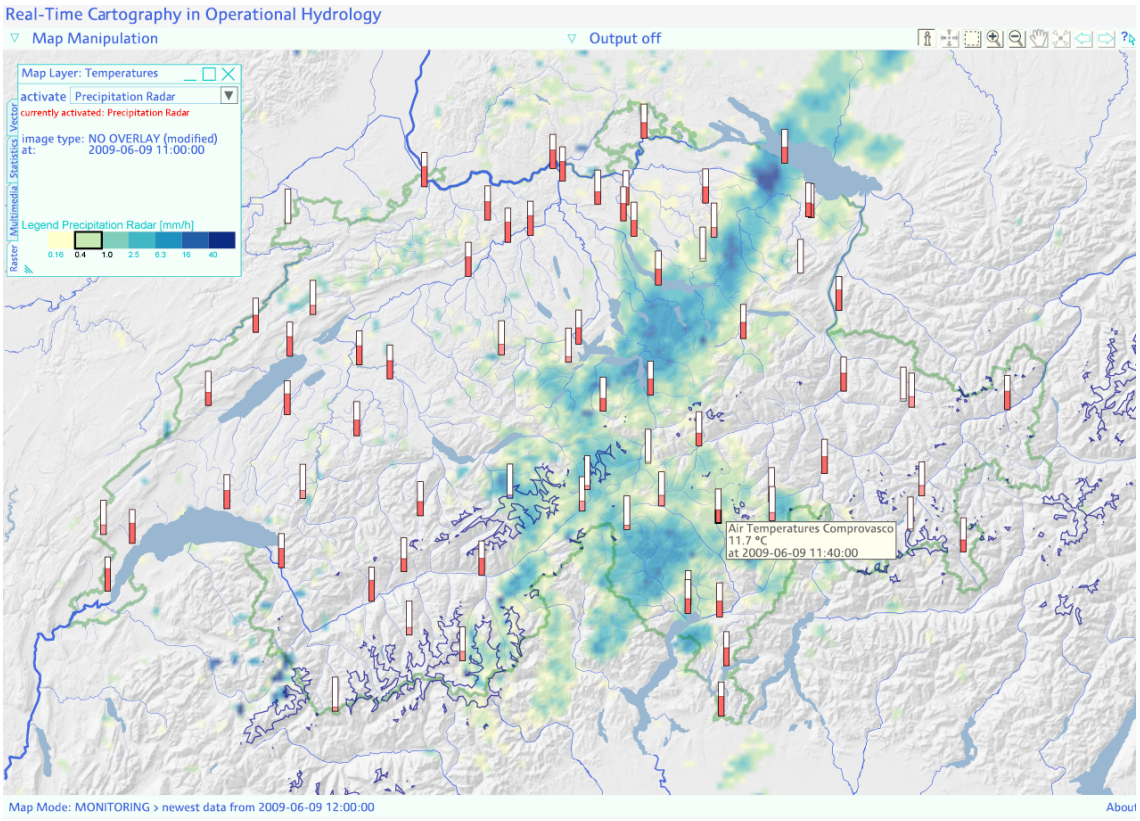

Fig. 4. Real-time map showing the modified precipitation radar image, temperature point data as framed-rectangle symbolization and the 0°C isotherm

4. Results

The cartographic results of the presented methods are accessible and visualized in an operational, web-based graphical user interface. Several examples are discussed in the following. In Fig. 4, a map is shown that contains the modified precipitation radar image, the framed rectangles for point temperature data and the 0°C isotherm. The

sequential color scheme and the reduced class number greatly facilitate the legibility of the quantitative data in the radar image. The framed rectangles of the various temperature gauges allow for a quick comparison of the data. When moving the mouse over such a rectangle, the precise gauge location name, temperature value and measurement time appear in tool tips next to the symbol. When moving the mouse over the radar image, the measurement time and the precipitation values appear in the ancillary window on top left. The mouse movement also triggers the display of the legend. Each time, the very class is being highlighted to which the actual mouse over value belongs. The map in Fig. 4 also points out that using isotherms is a sound way of overlapping temperature data with radar data. The spatial distribution of the area below 0°C overlapped by precipitation fields is presented to the user without compromising legibility.

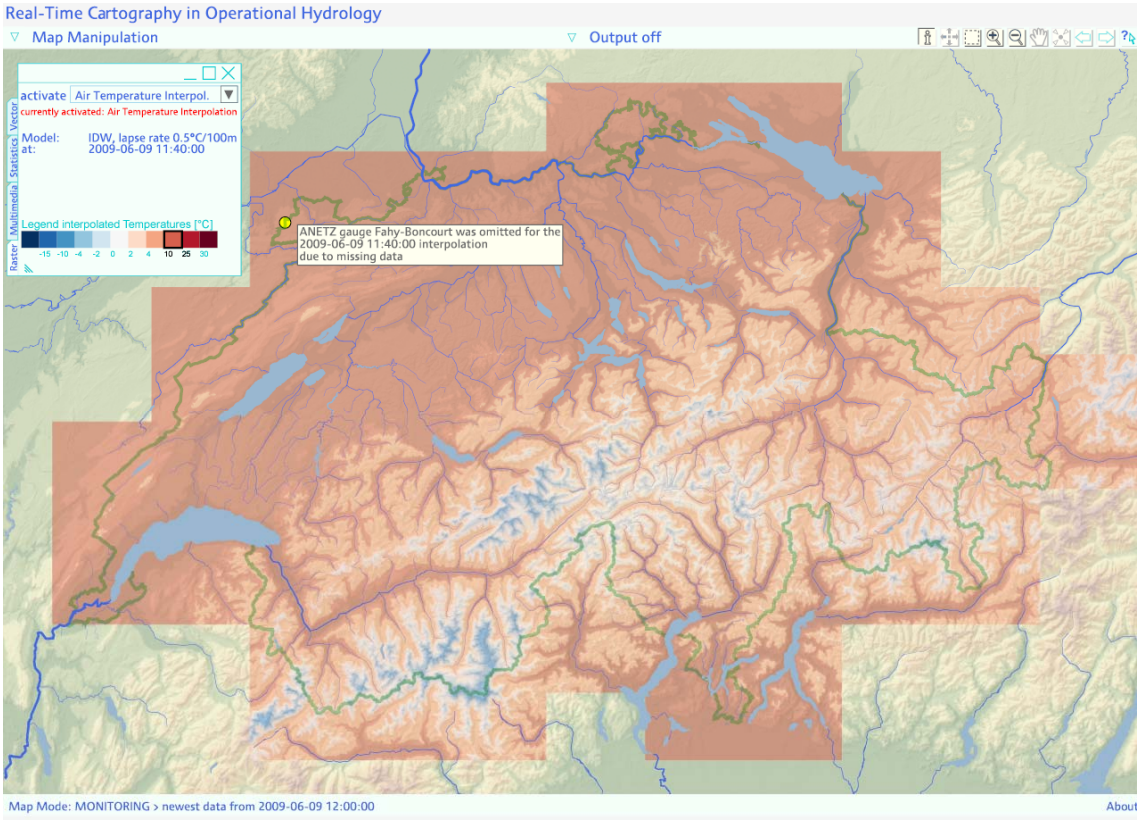

Fig. 5. Real-time interpolated temperature surface. Gauges left out for the interpolation are marked by a yellow dot.

The map of the automated real-time interpolation of temperature is shown in Fig. 5. The interpolation is performed on those tiles that cover Switzerland, omitting areas of bordering countries. A distinct diverging color scheme is applied to the interpolated data. The class intervals are irregular and smaller around the decisive 0°C. Again, data exploration of this raster image is facilitated when moving the mouse over it. The

temperature value and the adjusted legend are directly displayed in the window on the top left. The interpolated image is created in real-time using all available gauging locations (see location of the framed rectangles in Fig. 4). The interpolation function skips those gauges that fail to supply valid real-time data. Those gauges are marked with a yellow dot on the map.

The two map clippings in Fig. 6 show more clearly the smoothing effect of the bilinear resampling process of the precipitation radar image. The two examples also illustrate the facilitated, interactive data exploration. In the map on the left, the mouse is moved over a temperature gauge. Attribute and legend information are directly displayed in the window on the top left. The information disappears when moving away from the temperature symbol. Instead, the 0°C isotherm is highlighted and additional information on elevation and area are displayed (Fig. 6, right).

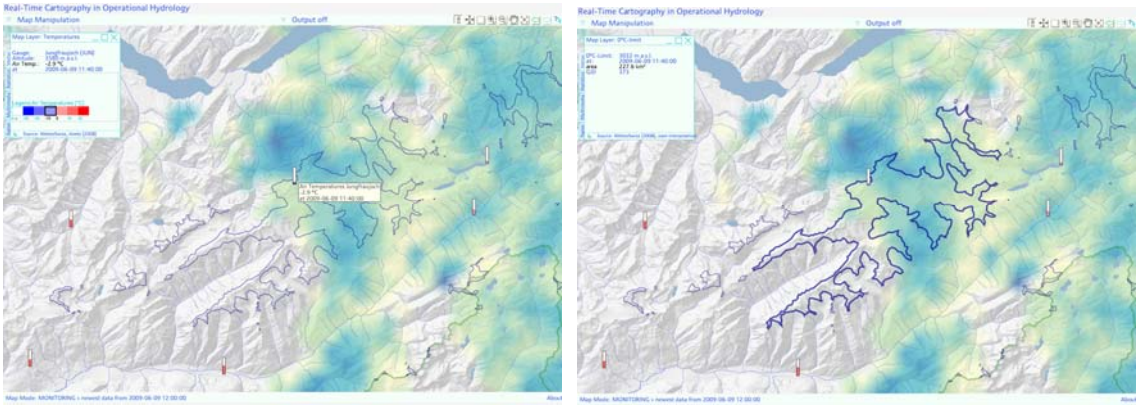

Fig. 6. Interactive exploration of temperature data (left) and 0°C-isotherm (right).

5. Discussion and Conclusions

Precipitation radar images on private or public weather service websites frequently fail to observe cartographic design rules. Results of the developed methods show that the shortcomings of inappropriate class numbers, illegible coloring or coarse resolution data can be visually addressed and improved in a real-time environment. Further working methods are introduced that improve the legibility of point temperature data. Complementary to point symbolization, automated real-time interpolation functions were successfully tested. They are capable of producing line and area temperature symbolization based on point data.

Both the radar and the interpolated temperature image are created and displayed using discrete color schemes, i.e., classified data. It might be argued that these parameters could be visualized just as well using color ramps and unclassified data. The decision in favor of the classified maps was made to allow for better and faster legibility and to test

interactive functions that link the maps symbols to highlighted legends. The developed interactive methods prove to facilitate exploration of both raster and vector data.

The presented real-time visualization and exploration improvements require fully automated and error-free processing. The main difficulty arises from the complexity of the workflows and – in case of temperature data – the data quality which is unknown in the first place. The latter problem is solved by checking the validity of the real-time values prior to their visualization. Gauges with faulty data are left out for subsequent work steps (i.e., visualization or interpolation).

The temperature interpolation is accomplished using an inverse distance weighted algorithm combined with an altitudinal lapse rate. It does not claim absolute accuracy as obvious problems arise when, for example, atmospheric inversion occurs, or when longitudinal lapse rates should be considered. This is often the case in Switzerland during *Foehn* winds, when 0°C levels in the north and south alpine part substantially differ. The accuracy of the interpolation model might be improved by the inclusion of daytime and season-dependent or even location-dependent lapse-rates. Integrating solar radiance may improve interpolation as well (see introduction). In this project, real-time radiation data are also collected, allowing for further possible research in this field.

Acknowledgments

This research is part of the PhD project "*Real-Time Cartography in Operational Hydrology*" and supported by the Swiss National Science Foundation (Grant No. 200020-122291). Special thank goes to Mr. S. Jaun for his help on the temperature interpolation and Mr. B. Jenny for his help on the precipitation radar image processing.

References

Antoniou, B., Tsoulos, L. (2006). The potential of XML encoding in geomatics converting raster images to XML and SVG. *Computers & Geosciences* 32(2): 184-194

Brewer, C.A., Hatchard, G.W., Harrower, M.A. (2003). ColorBrewer in Print: A Catalog of Color Schemes for Maps. *Cartography and Geographic Information Science* 30: 5-32

Cartwright, W. (2003). Maps on the Web. In: Peterson, M.P. (Ed.). Maps and the Internet. Amsterdam: Elsevier, pp 35-56

Chumchean, S., Seed, A., Sharma, A. (2006). Correcting of real-time radar rainfall bias using a Kalman filtering approach. *Journal of Hydrology* 317(1-2): 123-137

Chung, U., Yun, J.I. (2004). Solar irradiance-corrected spatial interpolation of hourly temperature in complex terrain. *Agricultural and Forest Meteorology* 126(1-2): 129-139

Fang, Z., Bedient, P.B., Benavides, J., Zimmer, A.L. (2008). Enhanced Radar-Based Flood Alert System and Floodplain Map Library. *Journal of Hydrologic Engineering* 13(10): 926-938

GDAL. (2009). "GDAL - Geospatial Data Abstraction Library". Retrieved June 12, 2009, from http://www.gdal.org/

Germann, U., Berenguer, M., Sempere-Torres, D., Zappa, M. (2009). REAL - Ensemble radar precipitation estimation for hydrology in a mountainous region. *The Quarterly Journal of the Royal Meteorological Society* 135(639): 445-456

Germann, U., Galli, G., Boscacci, M., Bolliger, M. (2006). Radar precipitation measurement in a mountainous region. *The Quarterly Journal of the Royal Meteorological Society* 132(618): 1669-1692

Haubrock, S., Dransch, D., Plattner, S. (2008). Delivering geospatial information with Web 2.0. In: Peterson, M.P. (Ed.). Maps in the Natural Disasters Networking Platform (NaDiNe) - Meeting user's needs: from static images to highly interactive real-time information integration. Berlin: Springer, pp 251-266

Hegg, C., Rhyner, J. (Eds.). (2007). Warnung bei aussergewöhnlichen Naturereignissen. Forum für Wissen. Swiss Federal Institute for Forest, Snow and Landscape Research: Birmensdorf

HIGRID. (2008). "Higrid - A class template that handles multi-resolution raster data". Retrieved June 12, 2009, from http://www.ika.ethz.ch/baer/programs/higrid/

Huang, S., Rich, P., Crabtree, R., Potter, C., Fu, P. (2008). Modeling Monthly Near-Surface Air Temperature from Solar Radiation and Lapse Rate: Application over Complex Terrain in Yellowstone National Park. *Physical Geography* 29(2): 158-178

Lienert, C., Weingartner, R., Hurni, L. (2007). Real-Time Cartography in Operational Hydrology. In: Proceedings of the 23rd International Cartography Conference, Moscow, Russia.

Lienert, C., Weingartner, R., Hurni, L. (2009). Real-Time Visualization in Operational Hydrology through Web-based Cartography. *Cartography and Geographic Information Science* 36: 45-58

MacEachren, A.M., Davidson, J.V. (1987). Sampling and Isometric Mapping of Continuous Geographic Surfaces. *Cartography and Geographic Information Science* 14: 299-320

Slocum, T.A. (2009). Thematic cartography and geographic visualization (third edition). Upper Saddle River, N.J.: Pearson-Prentice Hall

Szentimrey, T., Bihari, Z., Szalai, S. (2007). Comparison of Geostatistical and Meteorological Interpolation Methods. In: Dobesch, H. (Ed.). Spatial interpolation for climate data the use of GIS in climatology and meteorology. London: ISTE, pp 45-56

UMN. (2009). "Raster Data - MapServer 5.4.0 Documentation". Retrieved June 12, 2009, from http://mapserver.org/input/raster.html?highlight=bilinear#special-processing-directives

Valpreda, E. (2004). GIS and Natural Hazards. In: Casale, R., Margottini, C. (Eds.). Natural disasters and sustainable development. Berlin: Springer, pp 373-386

Wratt, D.S., Tait, A., Griffiths, G., Espie, P., Jessen, M., Keys, J., Ladd, M., Lew, D., Lowther, W., Mitchell, N., Morton, J., Reid, J., Reid, S., Richardson, A., Sansom, J., Shankar, U. (2006). Climate for crops: integrating climate data with information about soils and crop requirements to reduce risks in agricultural decision-making. *Meteorological applications* 13(4): 305-315